Journal of Coordination Chemistry

ISSN: 0095-8972 (Print) 1029-0389 (Online) Journal homepage: http://www.tandfonline.com/loi/gcoo20

Phenyl-functionalized diiron dithiolate complexes with one bidentate or two unidentate phosphine-containing ligands

Chang-Gong Li, Yong Zhu, Feng Xue, Mao-Jin Cui & Jing-Yan Shang

To cite this article: Chang-Gong Li, Yong Zhu, Feng Xue, Mao-Jin Cui & Jing-Yan Shang (2015) Phenyl-functionalized diiron dithiolate complexes with one bidentate or two unidentate phosphine-containing ligands, Journal of Coordination Chemistry, 68:13, 2361-2368, DOI: 10.1080/00958972.2015.1050006

To link to this article: http://dx.doi.org/10.1080/00958972.2015.1050006

Accepted author version posted online: 11 May 2015.
Published online: 05 Jun 2015.

Journal of Coordination Chemistry, 2015
Vol. 68, No. 13, 2361–2368, http://dx.doi.org/10.1080/00958972.2015.1050006

Phenyl-functionalized diiron dithiolate complexes with one bidentate or two unidentate phosphine-containing ligands

CHANG-GONG LI*, YONG ZHU, FENG XUE, MAO-JIN CUI and JING-YAN SHANG

College of Chemistry & Chemical Engineering, Henan Institute of Science and Technology, Xinxiang, PR China

(*Received 26 February 2015; accepted 20 April 2015*)

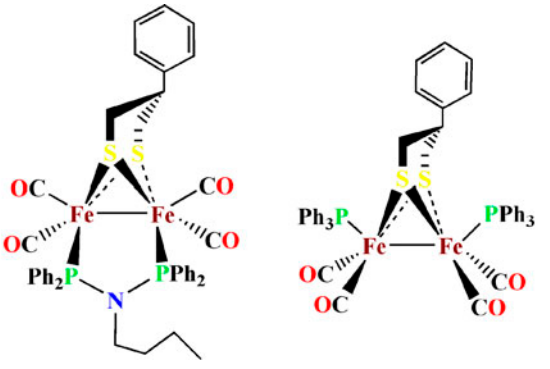

Treatment of diiron dithiolate complex, $[(\mu\text{-}SCH_2)_2CHC_6H_5]Fe_2(CO)_6$ (**A**), with one equivalent of bidentate phosphine-containing ligand *N*,*N*-bis(diphenylphosphine)butanamine $[(Ph_2P)_2N\text{-}Bu\text{-}n]$ in refluxing xylene afforded the diphosphine-bridged complex $[(\mu\text{-}SCH_2)_2CHC_6H_5]Fe_2(CO)_4[(\mu\text{-}PPh_2)_2N\text{-}Bu\text{-}n]$ (**1**) in high yield, while reaction of **A** with two equivalents of triphenylphosphine (PPh_3) in the presence of decarbonylating agent Me_3NO yielded the disubstituted complex $[(\mu\text{-}SCH_2)_2CHC_6H_5]Fe_2(CO)_4(PPh_3)_2$ (**2**) in low yield. Both complexes were characterized by spectroscopic methods and X-ray crystallography. In the solid state, two phosphines of $(PPh_2)_2N\text{-}Bu\text{-}n$ bridge the two irons with *cis* basal-basal conformation, while PPh_3 occupies an apical position of the square pyramidal geometries of each iron. The influence of coordination manner on the electrochemical properties of both complexes was investigated by cyclic voltammetry.

Keywords: [FeFe]-Hydrogenase; Diiron dithiolate complex; Phosphine ligand; Crystal structure; Electrochemistry

1. Introduction

Diiron dithiolate complexes have been a very interesting topic of research related to the biomimic chemistry of [FeFe]-hydrogenases [1–6]. Hydrogenases, discovered originally in enteric bacteria by Stephenson and Stickland in 1931, exist in a wide variety of organisms,

*Corresponding author. Email: lichanggong@sohu.com

such as bacteria, archaea, and some Eukarya and are divided into [NiFe], [FeFe], and [Fe]-hydrogenases on the basis of the metal composition of their active sites [7–10]. Among these enzymes, [FeFe]-hydrogenases catalyze the reversible interconversion between proton and molecular hydrogen, but are usually referred to as the catalytic evolution of hydrogen [11]. Following the depicted Fe/S clusters of the active sites of [FeFe]-hydrogenases by X-ray crystallography, diiron dithiolate complexes $[(\mu\text{-}SCH_2)_2X]Fe_2(CO)_6$ [X = CH_2, NH, O, S, CHOH, CHCOOH, NCH_2CH_2OH] and their derivatives were synthesized as models of the active sites of [FeFe]-hydrogenases, having insight into the catalytic mechanism and designing robust catalysts for production of hydrogen [1, 12–22]. As continuation of our efforts in phenyl-functionalized diiron dithiolate complexes, two disubstituted complexes with one bidentate or two unidentate phosphine-containing ligands were synthesized and the influence of coordination on the electrochemical properties was investigated by cyclic voltammetry [23–26].

2. Experimental

2.1. *Materials and methods*

All reactions and operations were carried out under a dry, oxygen-free argon atmosphere using standard Schlenk, and vacuum line techniques. CH_2Cl_2 and MeCN were distilled over CaH_2, while *n*-hexane, xylene, and toluene were distilled over sodium under argon. $Me_3NO{\cdot}2H_2O$ and PPh_3 were commercially available and used as received. Complex **A** and $(PPh_2)_2$-N-Bu-n were prepared according to literature methods [23, 27]. Preparative TLC was carried out on glass plates (25 cm × 20 cm × 0.25 cm) coated with silica gel G (10–40 μm). IR spectra were recorded on a Bruker TENSOR 27 FTIR spectrometer. ^1H and ^{31}P NMR spectra were obtained on a Bruker Avance 400 MHz spectrometer. Elemental analyses were performed on an Elementar Vario EL III analyzer.

2.2. *Electrochemistry*

Electrochemical measurements were carried out in a 10 mL one-compartment glass cell using a CHI 620 Electrochemical Workstation (CH Instruments, Chenhua, China). The electrolyte was *n*-Bu_4NPF_6 (0.1 M in MeCN), and the electrolyte solution was purged with dry nitrogen for 10 min before measurement. CV scans were obtained in a three-electrode cell with a glassy carbon electrode (3 mm diameter) as the working electrode, which was successively polished with 0.05 μm diamond paste, sonicated in ion-free water for 1 min, and then washed with acetone followed by air drying before usage. The auxiliary electrode was a platinum wire and the reference electrode was a nonaqueous Ag/Ag^+ electrode (0.001 M $AgNO_3$ and 0.1 M *n*-Bu_4NPF_6 in MeCN). The potential scale was calibrated against the Fc/Fc^+ couple and is reported *versus* this reference system.

2.3. *X-ray structure determination*

Single crystals of both complexes suitable for X-ray diffraction analysis were obtained by slow evaporation of *n*-hexane and dichloromethane solutions containing **1** or **2** at 4 °C. For each complex, a suitable crystal was mounted on an Xcalibur, Eos, and Gemini diffractometer.

Data were collected at 291.15 K. Using Olex2 [28], the structures were solved with the ShelXS structure solution program using direct methods and refined with the ShelXL refinement package using least squares minimization [29].

2.4. *Synthesis and characterization of 1*

A xylene (20 mL) solution of **A** (89 mg, 0.19 mmol) and $(PPh_2)_2$-N-Bu-n (84 mg, 0.19 mmol) were refluxed for 2 h under argon. The solvent was removed on a rotary evaporator and the residue was subjected to preparative TLC separation using CH_2Cl_2/petroleum ether (v/v = 1 : 1) as the eluent. Complex **1** was obtained as a red solid (140 mg, 87%). IR (KBr disk, cm^{-1}):$\nu_{C\equiv O}$ 1995 (vs), 1962 (s), 1925 (s). ^1H NMR (400 MHz, $CDCl_3$, ppm): 0.182 (m, 2 H, $NCH_2CH_2CH_2CH_3$), 0.284 (t, 3 H, $NCH_2CH_2CH_2CH_3$), 0.441 (m, 2 H, $NCH_2CH_2CH_2CH_3$), 1.829 (m, 2 H, 2 SH_aH_e), 2.550 (m, 1 H, CH), 2.673 (m, 2 H, 2 SH_aH_e), 2.795 (t, 2 H, $NCH_2CH_2CH_2CH_3$), 7.094 (s, 2 H, PhH), 7.459 (m, 19 H, PhH), 7.818 (m, 4 H, Ph*H*). ^{31}P NMR (161.9 MHz, $CDCl_3$, 85% H_3PO_4, ppm):119 (s). Anal. Calcd for $C_{41}H_{39}Fe_2NO_4P_2S_2$ (%): C, 58.10; H, 4.64; N, 1.65. Found: C, 57.86; H, 4.41; N, 1.52.

2.5. *Synthesis and characterization of 2*

To a MeCN (15 mL) solution of **A** (130 mg, 0.28 mmol) was added $Me_3NO{\cdot}2H_2O$ (62 mg, 0.56 mmol). The red solution became brown immediately. After stirring at room temperature for *ca*. 15 min, PPh_3 (147 mg, 0.56 mmol) in toluene (10 mL) was added and the mixture was stirred at room temperature for 3 h. After evaporation of solvents, the residue was subjected to preparative TLC separation using CH_2Cl_2/petroleum ether (v/v = 1 : 2) as eluent. From the brown band, **2** was obtained as a dark red solid (55 mg, 21%). IR (KBr disk, cm^{-1}): $\nu_{C\equiv O}$ 1990 (vs), 1953 (s), 1917 (m). ^1H NMR (400 MHz, $CDCl_3$, ppm): 1.74 (m, 3 H), 2.04 (m, 2 H), 6.55 (s, 6 H, Ph*H*), 7.41 (m, 29 H, Ph*H*). ^{31}P NMR (161.9 MHz, $CDCl_3$, 85% H_3PO_4, ppm): 61.4 (s). Anal. Calcd for $C_{49}H_{40}Fe_2O_4P_2S_2$ (%): C, 63.24; H, 4.33. Found: C, 63.01; H, 4.16.

3. Results and discussion

3.1. *Synthesis and spectroscopic characterization*

As shown in scheme 1, reaction of **A** with one equivalent of $(PPh_2)_2$-N-Bu-n in refluxing xylene afforded **1** in high yield, while treatment of **A** with two equivalents of PPh_3 in the presence of two equivalents of decarbonylating agent Me_3NO yielded **2** in low yield. The analogous disubstituted diiron dithiolate, dicobalt-iron or bridging diphosphine complexes were reported [24, 30–33]. The difference in yields for preparation of both complexes may be ascribed to the difference in steric demand of two ligands, as the Tolman cone angle of PPh_3 (145°) is larger than that of $(PPh_2)_2$-N-Bu-n (121°)[†] [34]. The substitution of phosphine for the first carbonyl assisted the displacement of the second carbonyl by phosphine

[†]Because $(PPh_2)_2$-N-Bu-n and bis(diphenylphosphine)methane have a similar backbone, we consider the Tolman cone angle of the former is close to that of the latter (121°) [34].

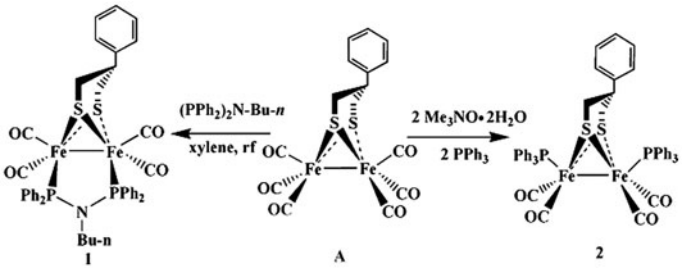

Scheme 1. Preparation of **1** and **2**.

in $(PPh_2)_2$-N-Bu-n due to construction of the rigid five-membered ring. The coordination manner was decided initially by IR [35]. The highest absorption frequency of the terminal carbonyls of **1** (1995 cm^{-1}) or **2** (1990 cm^{-1}) indicated that one carbonyl attached to each iron was replaced by phosphine simultaneously, as this frequency of the symmetrically disubstituted diiron complexes is close to, but less than 2000 cm^{-1} [24, 35]. The absorption frequencies of carbonyls in **2** were shifted to lower wave numbers compared with those of **1**, reflecting the higher electron density at diiron center and more back donation from iron to CO in **2**, ascribed to the better donor ability of PPh_3 than that of $(PPh_2)_2$-N-Bu-n [34, 36]. ^{1}H NMR spectrum of **1** showed up-field resonance signals in the range of 0.178–0.441 ppm for the propyl protons in butyl, while the resonance signal at 2.795 ppm was assigned to methylene attached to nitrogen. The resonance signals at 1.829, 2.550, and 2.673 ppm were assigned to protons of 1,3-propanedithiolate of **1**, whereas the counterparts in **2** were shifted up-field slightly, in accord with the higher electron density at diiron center in **2**. ^{31}P NMR spectrum of **1** displayed one singlet at 119 ppm, whereas that of **2** showed one singlet at 61.4 ppm [24, 30, 31].

3.2. *X-ray crystal structures*

Crystals of **1** or **2** suitable for X-ray crystallography were grown upon slow evaporation of *n*-hexane and dichloromethane solutions of **1** or **2**. The ORTEP views of both complexes are displayed in figures 1 and 2, while the crystal data and the selected metric data are given in tables 1 and 2, respectively. Each complex is composed of a [2Fe2S] core, in which the two irons are bridged by 1,3-propanedithiolate. The skeleton of 1,3-propanedithiolate and Fe2 in **1** or Fe1 in **2** constitute a six-membered ring in a chair conformation with phenyl group occupying an equatorial position. Two phosphines of $(PPh_2)_2$-N-Bu-n coordinate two irons of **1** in *cis* basal-basal manner, while the phosphine of PPh_3 occupies an apical position of the square pyramidal geometries of each iron. Fe1–Fe2–P2–N1–P1 constitute a five-membered ring in **1** with the dihedral angle 1.7 (1)° between planes (P1, N1, P2) and (P1, Fe1, Fe2), meaning that N1, P1, P2, Fe1, and Fe2 in the five-membered ring are almost co-planar. The Fe–Fe bond length of **1** [2.4914(10) Å] is close to those of $[(\mu\text{-}SCH_2)_2CHC_6H_5]Fe_2(CO)_4[(\mu\text{-}PPh_2)_2N\text{-}Pr\text{-}n]$ [2.4851(9) Å] [24] and (μ-PDT)$Fe_2(CO)_4[(\mu\text{-}PPh_2)_2N\text{-}Pr\text{-}n]$ [2.4836(11) Å] [30], whereas that of **2** [2.5496(9) Å] is almost the same as those of (μ-PDT)$Fe_2(CO)_4(PMe_2Ph)_2$ [2.5198(13) Å] [36], (μ-PDT)$Fe_2(CO)_4[P(OMe)_3]_2$ [2.5098(12) Å] [37] and the analogs [38].

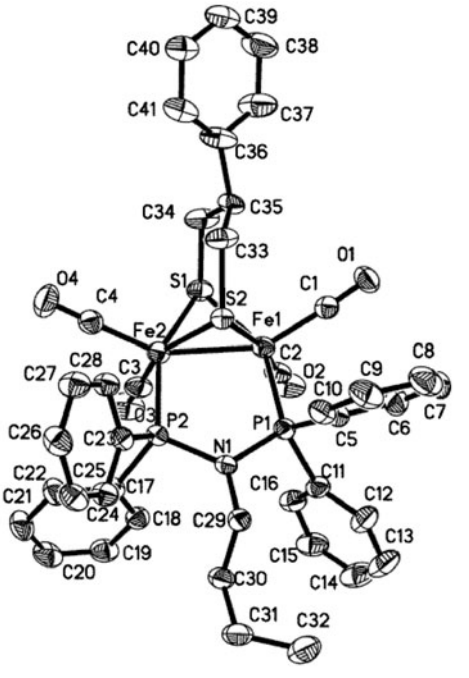

Figure 1. ORTEP view of **1** with 30% probability level ellipsoids.

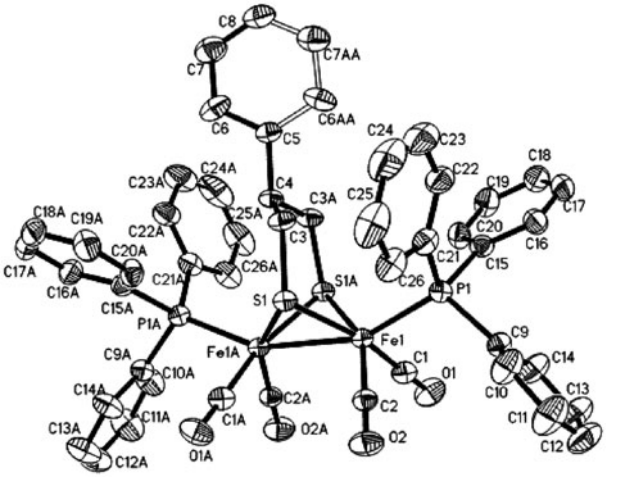

Figure 2. ORTEP view of **2** with 30% probability level ellipsoids.

3.3. *Electrochemistry*

Cyclic voltammetry of **1** or **2** was recorded in MeCN to observe the electrochemically induced reduction and oxidation properties (figure 3). A primary one-electron reduction with peak potential at –2.15 V for **1** or –2.11 V for **2** was observed, similar to that of

Table 1. Crystal data and structural refinements for **1** and **2**.

	1	**2**
Empirical formula	$C_{41}H_{39}Fe_2NO_4P_2S_2$	$C_{49}H_{40}Fe_2O_4P_2S_2$
Formula weight	847.49	930.57
Temperature (K)	291.15	291.15
Crystal system	Triclinic	Monoclinic
Space group	$P\bar{1}$	$C2/c$
a (Å)	10.9869(7)	15.9010(11)
b (Å)	12.7815(8)	15.5795(10)
c (Å)	15.4528(11)	18.2208(11)
α (°)	79.110(6)	90.00
β (°)	70.240(6)	95.927(6)
γ (°)	73.755(6)	90.00
Volume (Å^3)	1950.0(2)	4489.7(5)
Z	2	4
ρ_{calc} (g cm^{-3})	1.443	1.377
μ (mm^{-1})	8.082	7.069
F (0 0 0)	876.0	1920.0
Crystal size (mm^3)	0.1 × 0.08 × 0.08	0.18 × 0.16 × 0.14
2θ range for data collection (°)	6.12–130.14	7.96–134.16
Index ranges	$-12 \le h \le 12$	$-18 \le h \le 16$
	$-14 \le k \le 13$	$-13 \le k \le 18$
	$-16 \le l \le 18$	$-19 \le l \le 21$
Reflections collected	13,839	8067
Independent reflections (R_{int})	6426 [0.0504]	4016 [0.0317]
Data/restraints/parameters	6426/2/474	4016/23/294
Goodness-of-fit on F^2	0.972	1.031
Final R indexes [$I \ge 2\sigma(I)$]	$R_1 = 0.0509$, $wR_2 = 0.1039$	$R_1 = 0.0403$, $wR_2 = 0.1006$
Final R indexes [all data]	$R_1 = 0.0935$, $wR_2 = 0.1193$	$R_1 = 0.0504$, $wR_2 = 0.1074$
Largest diff. peak/hole/(e Å^{-3})	0.78/−0.30	0.34/−0.26

Table 2. Selected bond lengths (Å) and angles (°) for **1** and **2**.

1					
Fe(1)–Fe(2)	2.4914(10)	Fe(1)–P(1)	2.2148(13)	Fe(2)–P(2)	2.2169(13)
Fe(2)–S(1)	2.2494(14)	Fe(1)–S(2)	2.2561(12)	Fe(1)–S(1)	2.2528(14)
Fe(2)–C(4)	1.775(5)	P(1)–N(1)	1.720(3)	P(2)–N(1)	1.714(3)
Fe(2)–S(2)	2.2555(13)	Fe(1)–C(1)	1.768(5)	C(1)–O(1)	1.151(5)
S(1)–Fe(1)–Fe(2)	56.34(4)	Fe(1)–S(1)–Fe(2)	67.20(4)	P(1)–Fe(1)–Fe(2)	94.76(4)
S(2)–Fe(1)–Fe(2)	56.47(4)	Fe(1)–S(2)–Fe(2)	67.04(4)	P(2)–Fe(2)–Fe(1)	97.39(4)
S(2)–Fe(1)–S(1)	84.79(5)	S(2)–Fe(2)–Fe(1)	56.49(4)	N(1)–P(2)–Fe(2)	113.28(12)
S(1)–Fe(2)–S(2)	84.88(5)	S(1)–Fe(2)–Fe(1)	56.47(4)	N(1)–P(1)–Fe(1)	115.44(13)
C(1)–Fe(1)–Fe(2)	145.91(14)	C(4)–Fe(2)–Fe(1)	152.69(16)	P(1)–Fe(1)–C(1)	101.66(16)
2					
Fe(1)–Fe(1A)	2.5496(9)	Fe(1)–S(1A)	2.2716(8)	Fe(1)–S(1)	2.2602(8)
Fe(1)–P(1)	2.2468(8)	Fe(1)–C(1)	1.776(3)	Fe(1)–C(2)	1.765(3)
Fe(1A)–S(1)	2.2716(8)	O(1)–C(1)	1.143(4)	S(1)–C(3)	1.823(3)
S(1)–Fe(1)–S(1A)	83.65(3)	Fe(1A)–S(1)–Fe(1)	68.47(3)	S(1A)–Fe(1)–Fe(1A)	55.55(2)
P(1)–Fe(1)–Fe(1A)	154.70(2)	P(1)–Fe(1)–S(1A)	113.21(3)	P(1)–Fe(1)–S(1)	102.88(3)
C(1)–Fe(1)–S(1A)	86.59(10)	C(1)–Fe(1)–P(1)	92.66(11)	C(2)–Fe(1)–Fe(1A)	97.85(11)
S(1)–Fe(1)–Fe(1A)	55.98(2)	C(1)–Fe(1)–Fe(1A)	107.97(11)	C(2)–Fe(1)–S(1)	90.05(10)

$Fe_2(CO)_6(\mu\text{-}PPh_2)_2$ [33]. The oxidation potential at +0.35 V for **1** or +0.05 V for **2** was also assigned to a one-electron process. The assignment of one-electron reduction or oxidation is based on the electrochemistry of the reported analogs, along with comparison of the peak height with those of ferrocene measured under the same conditions. The redox of both complexes was shifted significantly toward cathode compared with those of **A** (reduction at –1.61 V, oxidation at +0.78 V) (figure 3), consistent with two carbonyls being replaced by

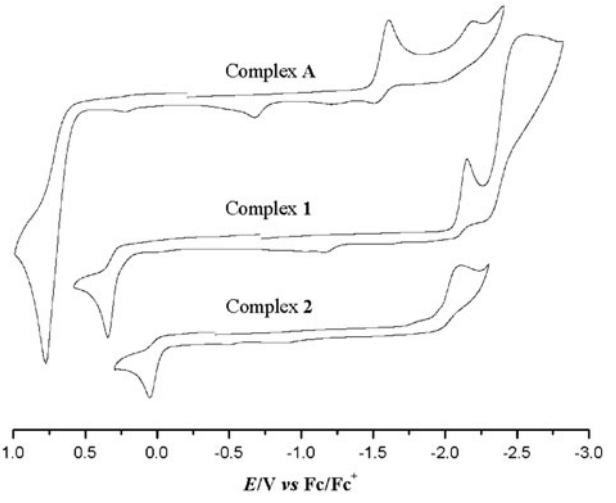

Figure 3. Cyclic voltammetry of **A**, **1** and **2** (0.001 M) in 0.1 M n-Bu_4NPF_6/MeCN at a scan rate of 0.1 V s^{-1}.

stronger electron-donating ligands [6]. The oxidation of **2** was shifted negatively compared with that of **1**, reflecting the higher electron density at diiron center of **2** and being consistent with the lower absorption frequencies in IR spectra [39]. However, reduction of **2** was shifted positively compared with that of **1**, indicating that **2** is ready to accept an electron. The rigidity of **1**, resulting from the rigid five-membered ring, hinders the rotation of the Fe–Fe bond and the structural reorganization after obtaining one electron, which are essential in the electrochemical reduction, while this structural reorganization may be favorable as two phosphines in **2** are not linked as in **1** [40, 41].

4. Conclusion

Substitution of one bidentate or two unidentate phosphine-containing ligands for two carbonyls in $[(\mu\text{-}SCH_2)_2CHC_6H_5]Fe_2(CO)_6$ yielded two symmetrically disubstituted complexes, $[(\mu\text{-}SCH_2)_2CHC_6H_5]Fe_2(CO)_4[(PPh_2)_2N\text{-}Pr\text{-}n]$ and $[(\mu\text{-}SCH_2)_2CHC_6H_5]Fe_2(CO)_4(PPh_3)_2$, respectively. The steric demand of ligand as well as the manner of coordination may influence the yield and redox properties. The investigations of electrochemistry of both complexes indicated that the electron density at the diiron center in **2** is slightly higher than that of **1** and subsequently the oxidation potential of **2** was shifted negatively as expected. However, the reduction potential of **2** was shifted positively, contrary to the higher electron density at the diiron center in **2**. The complex with bridging bidentate phosphine is readily prepared and stable in thermodynamics, but is unfavorable for reduction as it is not able to reorganize following the receipt of an electron.

Supplementary material

Crystallographic data for the structures reported in this article have been deposited with the Cambridge Crystallographic Data Center as supplementary publication Nos. CCDC 986639

(**1**) and 1041828 (**2**). Copies of the data can be obtained free of charge via www.ccdc.cam.ac.uk (or from the Cambridge Crystallographic Center, 12 Union Road, Cambridge CB21EZ, UK; Fax: +44 1223 336033; Email: deposit@ccdc.cam.ac.uk).

Disclosure statement

No potential conflict of interest was reported by the authors.

References

[1] C. Tard, C.J. Pickett. *Chem. Rev.*, **109**, 2245 (2009).
[2] F. Gloaguen, T.B. Rauchfuss. *Chem. Soc. Rev.*, **38**, 100 (2009).
[3] I.P. Georgakaki, L.M. Thomson, E.J. Lyon, M.B. Hall, M.Y. Darensbourg. *Coord. Chem. Rev.*, **238–239**, 255 (2003).
[4] W. Lubitz, H. Ogata, O. Rüdiger, E. Reijerse. *Chem. Rev.*, **114**, 4081 (2014).
[5] N. Wang, M. Wang, L. Chen, L.C. Sun. *Dalton Trans.*, **42**, 12059 (2013).
[6] G.A.N. Felton, C.A. Mebi, B.J. Petro, A.K. Vannucci, D.H. Evans, R.S. Glass, D.L. Lichtenberger. *J. Organomet. Chem.*, **694**, 2681 (2009).
[7] M. Stephenson, L.H. Stickland. *Biochem. J.*, **25**, 205 (1931).
[8] P.M. Vignais, B. Billoud, J. Meyer. *FEMS Microbiol. Rev.*, **25**, 455 (2001).
[9] P.M. Vignais, B. Billoud. *Chem. Rev.*, **107**, 4206 (2007).
[10] J.C. Fontecilla-Camps, A. Volbeda, C. Cavazza, Y. Nicolet. *Chem. Rev.*, **107**, 4273 (2007).
[11] M.W.W. Adams. *Biochim. Biophys. Acta*, **1020**, 115 (1990).
[12] J.W. Peters, W.N. Lanzilotta, B.J. Lemon. *Science*, **282**, 1853 (1998).
[13] Y. Nicolet, C. Piras, P. Legrand, C.E. Hatchikian, J.C. Fontecilla-Camps. *Structure*, **7**, 13 (1999).
[14] J.-F. Capon, F. Gloaguen, P. Schollhammer. *J. Talarmin. Coord. Chem. Rev.*, **249**, 1664 (2005).
[15] V. Artero, M. Fontecave. *Coord. Chem. Rev.*, **249**, 1518 (2005).
[16] M. Wang, L. Chen, L.C. Sun. *Energy Environ. Sci.*, **5**, 6763 (2012).
[17] X.M. Liu, S.K. Ibrahim, C. Tard, C.J. Pickett. *Coord. Chem. Rev.*, **249**, 1641 (2005).
[18] M. Rakowski DuBois, D.L. DuBois. *Chem. Soc. Rev.*, **38**, 62 (2009).
[19] T.R. Simmons, G. Berggren, M. Bacchi, M. Fontecave, V. Artero. *Coord. Chem. Rev.*, **270–271**, 127 (2014).
[20] J.F. Capon, F. Gloaguen, F.Y. Pétillon, P. Schollhammer, J. Talarmin. Coord. Chem. Rev., **253**, 1476 (2009).
[21] S. Ezzaher, J.F. Capon, N. Dumontet, F. Gloaguen, F.Y. Pétillon, P. Schollhammer, J. Talarmin. *J. Electroanal. Chem.*, **626**, 161 (2009).
[22] P.H. Zhao, K.K. Xiong, W.J. Liang, E.J. Hao. *J. Coord. Chem.*, **68**, 968 (2015).
[23] C.G. Li, Y. Zhu, X.X. Jiao, X.Q. Fu. *Polyhedron*, **67**, 416 (2014).
[24] C.G. Li, Y.F. Li, J.Y. Shang, T.J. Lou. *Transition Met. Chem.*, **39**, 373 (2014).
[25] C.G. Li, F. Xue, M.J. Cui, J.Y. Shang. *J. Cluster Sci.*, **25**, 1641 (2014).
[26] C.G. Li, F. Xue, M.J. Cui, J.Y. Shang, T.J. Lou. *Transition Met. Chem.*, **40**, 47 (2015).
[27] G. Ewart, A.P. Lane, J. McKechnie, D.S. Payne. *J. Chem. Soc.*, 1543 (1964).
[28] O.V. Dolomanov, L.J. Bourhis, R.J. Gildea, J.A.K. Howard, H. Puschmann. *J. Appl. Cryst.*, **42**, 339 (2009).
[29] G.M. Sheldrick. *Acta Cryst.*, **A64**, 112 (2008).
[30] L.C. Song, C.G. Li, J.H. Ge, Z.Y. Yang, H.T. Wang, J. Zhang, Q.M. Hu. *J. Inorg. Biochem.*, **102**, 1973 (2008).
[31] G.L. Newman, J.M.A. Rahman, J.B.G. Gluyas, D.S. Yufit, J.A.K. Howard, P.J. Low. *J. Cluster Sci.*, **26**, 233 (2015).
[32] L.J. Luo, X.F. Liu, H.Q. Gao. *J. Coord. Chem.*, **66**, 1077 (2013).
[33] Y.C. Shi, W. Yang, Y. Shi, D.C. Cheng. *J. Coord. Chem.*, **67**, 2330 (2014).
[34] C.A. Tolman. *Chem. Rev.*, **77**, 313 (1977).
[35] W.M. Gao, J. Ekström, J.H. Liu, C.N. Chen, L. Eriksson, L.H. Weng, B. Åkermark, L.C. Sun. *Inorg. Chem.*, **46**, 1981 (2007).
[36] P. Li, M. Wang, C.J. He, G.H. Li, X.Y. Liu, C.N. Chen, B. Åkermark, L.C. Sun. *Eur. J. Inorg.*, 2506 (2005).
[37] D. Morvan, J.-F. Capon, F. Gloaguen, P. Schollhammer. *J. Talarmin. Eur. J. Inorg. Chem.*, 5062 (2007).
[38] P. Li, M. Wang, C.J. He, X.Y. Liu, K. Jin, L.C. Sun. *Eur. J. Inorg. Chem.*, 3718 (2007).
[39] P.H. Zhao, X.H. Li, Y.F. Liu, Y.Q. Liu. *J. Coord. Chem.*, **67**, 766 (2014).
[40] S.J. Borg, J.W. Tye, M.B. Hall, S.P. Best. *Inorg. Chem.*, **46**, 384 (2007).
[41] P.E.M. Siegbahn, J.W. Tye, M.B. Hall. *Chem. Rev.*, **107**, 4414 (2007).